Fixed-Bed Multisolute Adsorption Characteristics of Nonwet Adsorbents

Certain nonfunctional macroreticular polymeric adsorbents are nonwet by sufficiently dilute aqueous solutions and enable separations not achievable with adsorbents in the prewet state. Fixed-bed adsorption data were obtained for a multisolute aqueous solution containing acetic acid, 1,3-butanediol, and succinic acid, with Porapak Q and Amberlite XAD-4 as adsorbents in both the prewet and nonwet states. The prewet breakthrough data agree with a model allowing for axial dispersion and a linear rate law, using independently estimated parameters. Breakthrough curves for the nonwet case depend strongly upon solute volatility since mass transport within the particles appears to occur by Knudsen diffusion, and is rate limiting. Data for Porapak Q reflect an effective particle diffusivity about ten times lower than for Amberlite XAD-4.

William G. Rixey, C. Judson King
Dept. of Chemical Engineering and
Lawrence Berkeley Laboratory
University of California
Berkeley, CA 94720

Introduction

Certain macroreticular polymeric adsorbents are nonwet by water, in the sense that air is not spontaneously displaced from the pores. Amberlites XAD-2 and XAD-4, poly(styrene-divinylbenzene) resins made by Rohm and Haas Corp., show this behavior, as does Ambersorb XE-340, a pyrolyzed sulfonated poly(styrene-divinylbenzene) resin manufactured by Rohm and Haas Corp. The factors controlling wetting of these resins by aqueous solutions have been analyzed (Rixey and King, 1988; Rixey, 1987). Conventional practice is for these resins to be prewetted before use by contacting them with a solvent such as methanol, followed by a water wash to remove the methanol. However, we have found that these adsorbents have interesting and potentially useful properties if left in the nonwet stage.

Even though they are nonwet by water and by dilute aqueous solutions of organic solutes, these resins do exhibit substantial adsorption capacities in the nonwet state. We have shown (Rixey and King, 1988; Rixey, 1987) that adsorption occurs as a surface-vapor equilibration. In order for adsorption to occur, an organic solute must vaporize at the interface between aqeous solution and pore vapor, and then diffuse along the pore to the adsorbing surface. In batch experiments carried out with several polar organic solutes (Rixey and King, 1987; Rixey, 1987) we have shown that the observed rates of adsorption of several organic solutes of differing volatility onto Amberlite XAD-4 in the nonwet state correspond to the rate-determining step being Knudsen diffusion of the solute along the pores.

Nonwet adsorbents have two potential advantages for recovery of organic solutes from aqueous solution:

1. Less water is taken up along with the solute by the adsorbent. The product recovered from the adsorbent is thereby more concentrated than for adsorption in the wetted state.

2. The rate of adsorption is directly proportional to the volatility of the solute over the aqueous solution. Therefore it should be possible to fractionate among solutes differing substantially in volatility, even though these solutes would not be separated by conventional adsorption in the wetted state.

There are also potential disadvantages of nonwet adsorbents:

1. The rate of adsorption is less than that in the wetted state, except for solutes of very high volatility.

2. The adsorption capacity is often less than that in the wetted state. However, we have shown criteria by which adsorbents can be chosen so as to reduce or even eliminate this difference (Rixey and King, 1988; Rixey, 1987).

3. The regeneration process must be one that returns the adsorbent to the nonwet state for reuse. One possibility, which we have shown to be effective (Rixey, 1987), is regeneration by leaching with a volatile solvent, followed by draining and vaporization of residual solvent.

The goal in the research presented here was to investigate fixed-bed adsorption behavior for multisolute aqueous mixtures for both the nonwet and conventional prewet states. Subsidiary goals were to demonstrate separation capability for solutes dif-

Correspondence concerning this paper should be addressed to C.J. King.
The present address of W.G. Rixey is Henkel Research Corp., Santa Rosa CA 95407.

fering in volatility, and to rationalize the observed breakthrough behavior quantitatively in terms of underlying concepts.

Experimental Methods

Materials

Porapak Q (Waters Associates, Division of Millipore Corp.) was chosen as the primary packing material for the fixed-bed studies. The small particle size of Porapak Q (about 150 μm) was desirable in order to obtain relatively sharp breakthrough curves for adsorption of solutes in the nonwet state. In addition, a fixed-bed, nonwet adsorption experiment was carried out with Amberlite XAD-4, the adsorbent used in the previous batch experiments (Rixey and King, 1987).

Properties of Porapak Q and XAD-4 are shown in Table 1. The surface area for XAD-4 was measured with a Model 201 BET Surface Area Analyzer (Porous Materials, Inc., Ithaca NY). Sources for the values reported for Porapak Q are given by Rixey (1987). The pore volume was measured by helium displacement for XAD-4 and by nitrogen adsorption for Porapak Q.

Apparatus

Fixed-bed runs were carried out in a polycarbonate (Lexan, General Electric Co.) column, 1.5 cm ID × 50 cm length. Polycarbonate was used as the column material in order to reduce channeling near the wall of the column due to preferential wetting effects. The column was equipped with glass inlet and outlet fittings. Aqueous feed solutions and solvent were pumped upward through the column by means of a Microflow Pulsafeeder metering pump (Interface Corporation, Lapp Insulator Division), at flow rates that ranged from 0.25 to 2 mL/min. Effluent samples were collected with an LKB 2211 SuperRac fraction collector (LKB-Produkter AB).

Samples were analyzed with a Spectra-Physics SP8000B High Performance Liquid Chromatograph, equipped with an RCM-100 Radial Compression Module (Water Associates, Inc.). Solutes were detected with a Model R401 Differential Refractometer (Waters Associates, Inc.). The mobile phase used for analysis was a pH 2 aqueous solution of sulfuric acid. Two columns were used: a reverse-phase Radial-Pak μ-Bondapak C-18 column with 5 μm particles (Waters Associates, Inc.), and an Aminex HPX-87H column (Bio-Rad Laboratories), a strong cation-exchange column in the hydrogen form.

Bed preparation

Prior to the first fixed-bed experiment, the column was filled with acetone by means of a 50 mL separatory funnel attached to the top of the column. Untreated Porapak Q was loaded into the column as a slurry in acetone, in order to ensure that air was not present in the adsorption column as either air within the pores of the particles or air trapped within the interstices of the particles.

Table 1. Properties of Amberlite XAD-4 and Porapak Q

	XAD-4	Porapak Q
BET nitrogen surface area, m^2/g	760	530–655
Pore volume, mL/g	0.99	1.2
Skeletal density, g/mL	1.09	—
Particle size (U.S. sieve series)	20–50	80–100

The bed was filled to a height of 45 cm and was supported by glass wool at both ends.

The Porapak Q column was then washed with acetone at a flow rate of 2 mL/min. Several 1 mL samples were periodically collected at the column effluent and analyzed by liquid chromatography with the C-18 column in order to monitor the concentrations of the impurities desorbing from the Porapak Q particles.

Peaks corresponding to ethyl-vinylbenzene, styrene, and divinylbenzene were monitored. The washing step was continued until impurities in the samples could no longer be detected. The minimum concentration for detection was estimated to be approximately 1 ppm. Three bed volumes of acetone were required to achieve this level of concentration. An additional two bed volumes of acetone were passed through the bed to insure that the bed was adequately solute-free.

Acetone was then allowed to drain freely from the bed. Distilled water, further treated by a Milli-Q Water Purification System (Millipore Corp.), was then fed to the column at 2 mL/min. The effluent concentration was sampled and analyzed for acetone by liquid chromatography with the C-18 column until acetone was no longer detected. This corresponded to approximately three bed volumes of water. An additional two bed volumes of water were passed through the bed to insure that the bed was free of all solutes.

Prewet Adsorption with Porapak Q

Procedure

A multisolute mixture consisting of 0.5 wt. % each of acetic acid, 1,3-butanediol, and succinic acid was introduced into the prewet bed at a flow rate of 0.25 mL/min. These three solutes were chosen as model solutes because they have very different volatilities but were expected to have similar equilibrium adsorption capacities on nonfunctionalized adsorbents. Estimates of the volatilities over aqueous solution and the activity coefficients are given elsewhere (Rixey, 1987).

The column effluent was routed to a fraction collector, which collected successive 2.5 mL samples. Every other sample was analyzed by liquid chromatography with the Aminex column.

Experimental breakthrough curves

The breakthrough curves for each of the three solutes are shown in Figure 1 as the ratio of the effluent concentration to the feed concentration for each solute vs. the volume of effluent collected. Data points are shown for 5 mL increments. Since 2.5 mL samples were collected and every other sample analyzed, each data point of Figure 1 represents an average concentration for a 2.5 mL increment.

Using 0.31 g/cm^3 of bed volume as the bulk particle density for Porapak Q (Rixey, 1987), the weight of an 80 mL bed of Porapak Q particles is 25 g. From Figure 1 the breakthrough acetic acid concentration is 50% of the feed concentration at an effluent volume of 118 mL. This value includes the interstitial volume of the bed, which is approximately 35 mL. The amount of acetic acid adsorbed onto the column is therefore approximately (118 − 35) g × 0.005 g acid/g solution = 0.415 g, assuming a liquid density of 1.00 g/mL. Thus the capacity is 0.017 g acetic acid/g adsorbent, in good agreement with 0.015 g/g determined from equilibrium measurements on Amberlite XAD-2 and XAD-4 (Rixey and King, 1988).

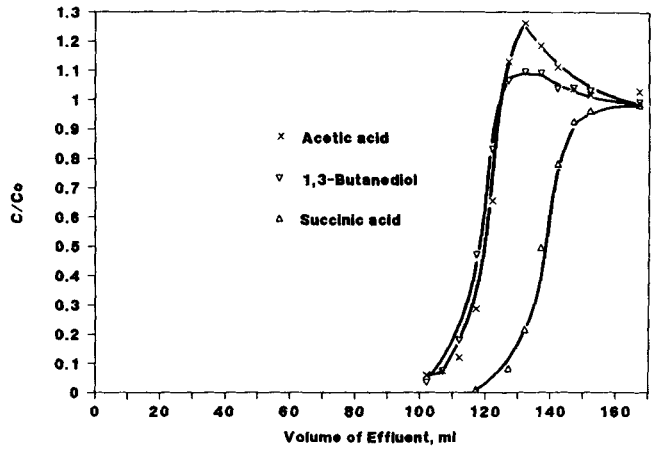

Figure 1. Breakthrough curves for a multisolute aqueous solution adsorbing onto prewet Porapak Q.

In addition to providing a measure of the capacity for solutes, the breakthrough curves can also be used to determine rate effects. Figure 1 shows that the sharpness of the breakthrough curves is similar for the three solutes. This is the expected result if external boundary-layer mass transfer, intraparticle diffusion, and/or axial dispersion control the rate of adsorption, since the molecular liquid-phase diffusivities and the dispersion coefficients are roughly the same for the three solutes. Further analysis is needed to determine which one or more of these mechanisms is rate determining.

The breakthrough curves for acetic acid and 1,3-butanediol in Figure 1 exhibit maxima that are higher than the feed concentration, while the breakthrough curve for succinic acid exhibits simple S-shaped behavior. These maxima reveal competitive adsorption among the solutes (Ruthven, 1984).

Prediction of breakthrough curves

The theory for predicting fixed-bed breakthrough curves has been summarized by Ruthven (1984). A full solution requires a complicated numerical solution, allowing for convective transport in the bulk fluid, axial dispersion, mass-transfer resistance external to the particles, and transport within the particles, even if adsorption kinetics are assumed not to provide a significant rate limit.

The most commonly used simplification avoids the complexity of solving the partial differential equation for intraparticle diffusion by using the approximation of a linear driving force model (Glueckauf and Coates, 1947). Diffusion within the particles is accounted for as an intraparticle resistance, which is combined with the external boundary-layer resistance into a lumped rate constant, k (s^{-1}), where (Ruthven 1984):

$$\frac{1}{k} = \frac{R_p}{3k_f} + \frac{R_p^2}{15D_p} \tag{1}$$

Here and subsequently, the particles are assumed to be spherical, with uniform radius.

Lapidus and Amundson (1952) obtained the following analytical expression for the breakthrough curve for the case of a linear or linearized isotherm:

$$\frac{C}{C_o} = \exp\left(\frac{vz}{2D_L}\right)\left[F(t) + \frac{k}{K}\int_o^t F(t)\,dt\right] \tag{2}$$

where

$$F(t) = e^{-kt}\int_o^t I_o\left[2k\sqrt{\frac{1-\epsilon}{K\epsilon}u(t-u)}\right]\frac{z}{2\sqrt{\pi D_L u^3}} \cdot \exp\left(\frac{-z^2}{4D_L u} - \frac{v^2 u}{4D_L} - ku\frac{1-\epsilon}{\epsilon} + \frac{ku}{K}\right)du \tag{3}$$

An algorithm for the integration of Eq. 2 is presented elsewhere (Rixey, 1987).

For the conditions of Figure 1, $R_p = 0.0075$ cm and the flow rate was 0.25 mL/min. The total bed volume of 80 mL, interstitial bed volume of 35 mL, and bed length of 45 cm yield $v = 0.0054$ cm/s and a superficial velocity of 0.0023 cm/s. Assuming a fluid viscosity of 1 mPa · s and a fluid density of 1.00 g/cm^3 yields a particle Reynolds number of 0.0035 based on the superficial velocity. For this Reynolds number the axial particle Peclet number ($Pe_p = vd_p/D_L$) is estimated from literature correlations (Sherwood et al., 1975) to be about 0.30, which in turn corresponds to $D_L = 0.00027$ cm^2/s. The axial Peclet number based on the length of the bed, $Pe_b = Pe_p z/d_p$, is therefore estimated as 900 for this set of values.

The external film mass transfer coefficient, k_f, can be estimated from the following equation (Sherwood et al., 1975):

$$\frac{k_f d_p}{D_f} = 4 + 1.21\,Pe_p^{2/3} \tag{4}$$

Taking a value for D_f of 1×10^{-5} cm^2/s yields a value for k_f of 0.0020 cm/s.

Assuming that the ratio of particle porosity to tortuosity is the same as that found for Amberlite XAD-4 (Rixey, 1987), the effective intraparticle diffusivity, D_p, is estimated to be 0.19 times the fluid-phase diffusivity, D_f.

Substituting numerical values for the terms on the righthand

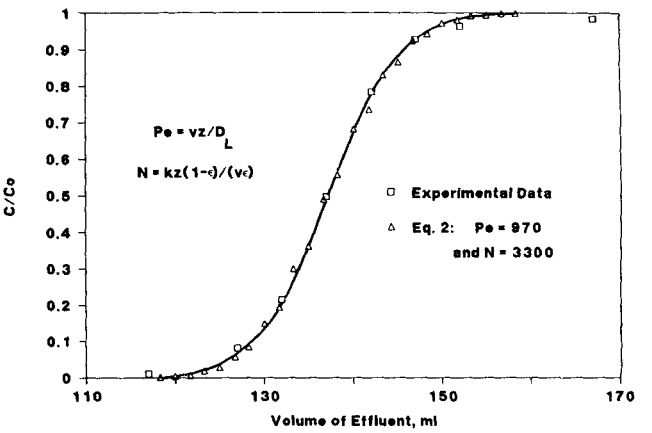

Figure 2. Axial dispersion plus linear rate law model, Eq. 2, fitted to succinic acid breakthrough curve for conditions of Figure 1.

side of Eq. 1 now yields:

$$\frac{1}{k} = 1.3 + 2.0\ (s^{-1}) \tag{5}$$

which indicates that particle diffusion and external mass-transfer resistance are both important, with particle diffusion somewhat more so.

A breakthrough curve calculated from Eq. 2 is plotted in Figure 2 along with the succinic acid breakthrough data of Figure 1. As the trailing breakthrough curve, that for succinic acid should be relatively free of multicomponent displacement effects. The capacity of the bed for succinic acid is about 22 mg/g, or about 7.5% of a monolayer. Abe et al. (1983) report isotherms for ethyl acetate, 2-pentanone, and 2-butanone onto Amberlite XAD-4, a chemically similar adsorbent, in the same loading range. From their results a linear isotherm is a reasonable approximation. A value of $K = 2.3$ for succinic acid on prewet Porapak Q was used, determined from the 50% breakthrough point of Figure 1. A value of 3,300 for the number of transfer units, N, was estimated where N is defined as:

$$N = kz\,\frac{1-\epsilon}{v\epsilon} \tag{6}$$

Use of $Pe_b = 970$ provides the best fit to the experimental data. This value agrees well with the value of 900 estimated above.

The close agreement between the experimental and predicted breakthrough curves for this prewet Porapak Q experiment indicates that additional effects, such as preferential channeling at the walls, are not significant.

Nonwet Adsorption with Porapak Q

Batch rate experiments with nonwet Amberlite XAD-4 showed that the rate of intraparticle diffusion was directly related to the volatility of a solute over aqueous solution (Rixey and King, 1987). For acetic acid, the rate of adsorption on nonwet XAD-4 was found to be 25 times slower than if the pores were filled with liquid, that is, than the prewet adsorption case. Thus the intraparticle resistance term in Eqs. 1 and 5 should increase by a factor of 25, and intraparticle diffusion should broaden the breakthrough curve relative to the prewet case. 1,3-butanediol, which is less volatile still, would be expected to have an even broader breakthrough curve.

Procedure

After the prewet adsorption experiment, the bed was regenerated with ethanol. The results of the regeneration are discussed elsewhere (Rixey, 1987). The bed was then dried with air at a flow rate of approximately 10 mL/s for 36 h in order to ensure that the particles were sufficiently free of solvent prior to a nonwet adsorption run.

In preliminary experiments it was found that interstitial air was not fully displaced if an experiment was simply started with upflow of aqueous feed into the dry bed.

In order to insure that all of the air was displaced from the interstices of the column, an additional glass column was attached to the bottom of the polycarbonate column. The glass column was filled with the Porapak Q adsorbent particles, while the polycarbonate column was initially empty. Solute-free water was introduced into the glass column until both the glass column and the polycarbonate column were filled with water. The adsorbent particles floated to the top of the polycarbonate column, since the particles contained air within the pores. Water was then introduced in downflow from the top of the polycarbonate column at a flow rate sufficient to fluidize the adsorbent particles and dislodge trapped interstitial air. The glass column attached to the polycarbonate column provided the additional volume necessary for fluidization.

The flow was then reduced to allow the resin particles to pack evenly in the polycarbonate column. Both sections were immersed in a large reservoir of water, and the polycarbonate column was detached from the glass column under the surface of the reservoir so as to keep the column packing within the upper polycarbonate column. The inlet column fittings were reattached to the adsorption column, and the column was ready for additional fixed-bed experiments.

An aqueous feed solution of the same composition as in the prewet case was introduced into the column at the same flow rate, 0.25 mL/min. As soon as effluent appeared, the collection of samples was initiated. Samples of 2 mL volume were collected in succession and analyzed in the same manner as described for the prewet adsorption experiment.

Experimental breakthrough curves

The breakthrough curves for the three solutes are shown in Figure 3. In contrast to the results for the prewet adsorption experiments, the sharpnesses of the breakthrough curves are significantly different for different solutes, and the relative positions are different. Acetic acid, which is the most volatile of the three solutes, has a sharper breakthrough curve than 1,3-butanediol. 1,3-butanediol adsorbs; however, its breakthrough curve is quite broad. The succinic acid breakthrough curve should be a measure of axial dispersion and/or channeling in the adsorption column, since the volatility of succinic acid is too low to allow significant adsorption given the residence time of the adsorption experiment.

Note that the sharpness of the breakthrough curve for acetic acid in the nonwet case approaches that for the prewet case, Fig 1. A comparison of the breakthrough curves of acetic acid in Figures 1 and 3 also shows that the adsorption capacity in the nonwet state is about four times less than that in the prewet

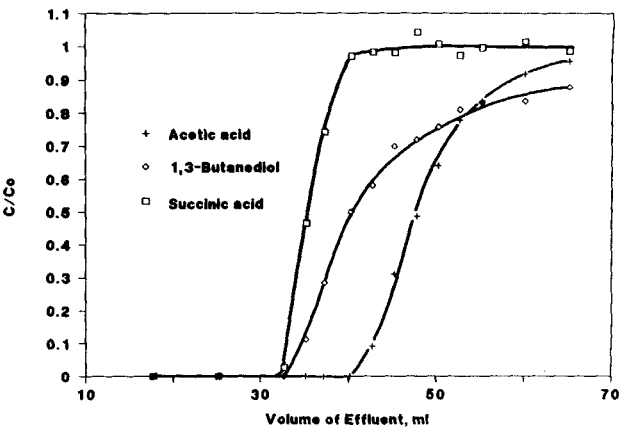

Figure 3. Breakthrough curves for nonwet Porapak Q, with column interstices initially full of solute-free water.

state. This result is consistent with equilibrium adsorption measurements on Amberlite XAD-2 (Rixey and King, 1988).

Interpretation of breakthrough curves

Using $Pe_b = 970$, as was found in the prewet case, Figure 2, a breakthrough curve was calculated using Eq. 2 with a value of $N = 0$. As shown in Figure 4, this curve fits the succinic acid data well. This is a good indication that additional effects, such as channeling, are not significant in the nonwet case.

The breakthrough curves for 1,3-butanediol and acetic acid were modeled with Eq. 2. Using $Pe_b = 970$ and $K = 0.30$ for acetic acid, a breakthrough curve for $N = 20$ was calculated and is shown in Figure 4. A value of $K = 0.3$ provided the best fit to data. Overall, a reasonably good fit to the data is observed. The value of 20 for N is more than a factor of 10 less (Rixey, 1987) than expected from the batch rate experiments for XAD-4 particles (Rixey and King, 1987). Note that this is the best fit to all of the data for acetic acid; using $N = 20$ underestimates the sharpness of the leading edge of the experimental breakthrough curve and overestimates the sharpness of the trailing edge. The leading edge could be characterized by a higher value of N. It is less likely that the shape of the leading edge could be ascribed to a nonlinear, favorable isotherm. Although we did not measure equilibrium adsorption data in the concentration range 0–0.5 wt. % for Porapak Q, data for adsorption of acetic acid on Amberlite XAD-2 suggest a linear isotherm for the concentration range from 0.02 to 0.5 wt. % (Hasanain and Hines, 1981). (The experiments of Hasanain and Hines appear to have been inadvertently carried out in the nonwet state.) XAD-2 and Porapak Q would be expected to behave similarly.

Using an axial Peclet number of 970 and an equilibrium constant of 0.18 for 1,3-butanediol (Rixey and King, 1988), a breakthrough curve for $N = 1$ was calculated. This value of K was determined from the ratio of adsorption densities for 1,3-butanediol and acetic acid determined from batch equilibrations for XAD-4 (Rixey, 1987), multiplied by the value of $K = 0.3$ for acetic acid on Porapak Q. The calculated curve is shown along with the breakthrough data for 1,3-butanediol in Figure 4. Again, reasonably good agreement with experimental data is observed. This value for N is 20 times lower than the best fit to the acetic acid breakthrough curve. This factor of 20 is in qualitative agreement with the factor of 25 estimated by Rixey and King (1987) for the ratio of the rates of adsorption. Note that the linear rate law applied to intraparticle diffusion within spherical particles begins to break down as N approaches 1 (Rixey, 1987). However, because of the effect of axial dispersion in the column, the differences in the calculated breakthrough curves for 1,3-butanediol using the linear rate law model and the intraparticle diffusion model are expected to be small.

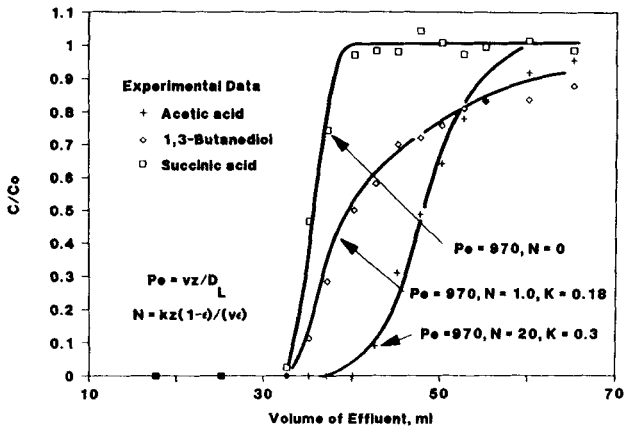

Figure 4. Axial dispersion plus linear rate law model, Eq. 2, fitted to multisolute breakthrough curves for nonwet Porapak Q, conditions of Figure 3.

To summarize the results for adsorption onto Porapak Q:

1. The axial dispersion plus linear rate law model, with the assumption of linearized equilibrium, provides a good fit to the breakthrough data for all of the solutes.
2. The succinic acid breakthrough curve is a measure of axial dispersion in the column. The axial Peclet number obtained from the model is in good agreement with literature estimates and the prewet experimental results, thereby indicating that preferential channeling in the column, when it is initially filled with solute-free water, is not significant.
3. Using the Peclet number obtained from the succinic acid curve, the model was used to determine independently the effects of mass transfer on the breakthrough curves for acetic acid and 1,3-butanediol. Acetic acid diffuses into the particles at a rate 20 times greater than 1,3-butanediol, as expected from earlier results. However, the intraparticle rate of diffusion, corrected for differences in particle sizes, is roughly a factor of 10 lower than that obtained from the batch rate experiments for Amberlite XAD-4.

Breakthrough Curves for Nonwet Amberlite XAD-4

A fixed-bed adsorption experiment with a multisolute aqueous solution was carried out with a column of Amberlite XAD-4 particles. The purpose was to determine whether the apparent lower than expected N characterizing the breakthrough curves for nonwet Porapak Q could be due to differences in the properties of Porapak Q and Amberlite XAD-4.

The following experimental conditions were used: flow rate = 0.67 mL/min, which corresponds to $v = 0.014$ cm/s; $z = 19$ cm; and $C_o = 0.5$ wt. % for each of two solutes, acetic acid and 1,3-butanediol. Because of the larger particle size for XAD-4 (0.05 cm dia. vs. 0.15 mm for Porapak Q) and the higher velocity and shorter bed length, the breakthrough curves are broader than those for the Porapak Q experiment. Assuming that Porapak Q and XAD-4 provide equal effective diffusivities, from Eq. 6 the value of N characterizing the intraparticle diffusion for a solute in this experiment was expected to be 70 times lower than that for the Porapak Q experiment.

The experimental breakthrough curves are shown in Figure 5 along with curves calculated using Eq. 2. The curves are broader than those of Figure 4, as expected. The model of axial dispersion plus a linear rate law was used with an axial Peclet number of 125, based upon the axial Peclet number of 970 for the Porapak Q results, corrected for the differences in the particle diameters and the bed lengths. This model provides a good fit to the acetic acid breakthrough curve, characterized with a value of $N = 2.5$. This value of N is only eight times smaller than that for acetic acid in the Porapak Q experiment, not the factor of 70 anticipated assuming that the effective particle diffusivities are the same for the two adsorbents. Thus, acetic acid appears to diffuse into the XAD-4 particles with an effective diffusivity which is (70/8 =) almost nine times greater than that inferred

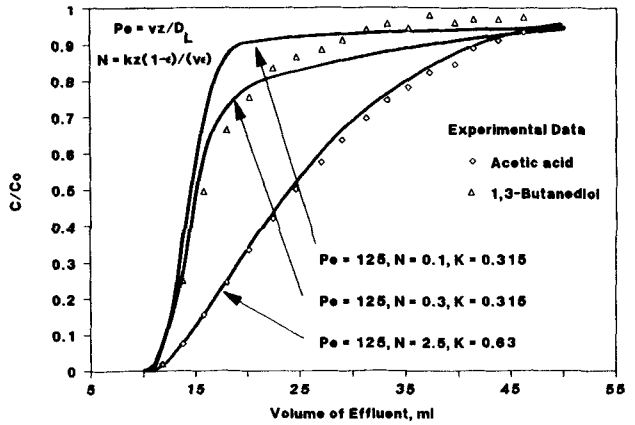

Figure 5. Axial dispersion plus linear rate law model, Eq. 2, fitted to multisolute breakthrough curves for nonwet Amberlite XAD-4.

for Porapak Q. This result is consistent with the interpretation of the batch rate data for XAD-4 presented previously (Rixey and King, 1987). An equilibrium constant of 0.63 for acetic acid obtained from the fixed-bed breakthrough curve agrees with the equilibrium measurements presented elsewhere (Rixey and King, 1988), was used for the calculated curve in Figure 4.

Equation 2 does not provide as good a fit to the 1,3-butanediol data. Shown in Figure 5 are curves calculated for $N = 0.1$ and 0.3. The shapes of the curves for these low values of N are influenced significantly by the value of K. A value of 0.315 taken from batch equilibration data reported previously (Rixey, 1987) has been used here. Another possible explanation for the inability to fit the data well is the use of the linear driving force approximation for these low values of N. The linear rate law model predicts a broader breakthrough curve than the intraparticle diffusion model for low values of N. This fact agrees qualitatively with Figure 5, where Eq. 2 predicts a broader breakthrough than the experimental data show.

Despite the inability of Eq. 2 to provide a good fit to the data, the values of $N = 0.1$ and 0.3 used with Eq. 2 do appear to bracket the actual number of transfer units for 1,3-butanediol in this experiment. The rate of adsorption is, therefore, roughly 8 to 25 times lower than that for acetic acid. The value of 25 is more consistent with the nonwet XAD-4 batch rate data (Rixey and King, 1987) and the nonwet Porapak Q fixed-bed results. Thus, modeling of the 1,3-butanediol breakthrough curve supports the conclusion from the acetic acid data that the intraparticle diffusion rate for XAD-4, corrected for particle size, is at least an order of magnitude greater than that for Porapak Q.

One way to explain this difference is in terms of a lower effective intraparticle diffusivity. The Porapak Q particles used in this study could have a pore size distribution which is much broader than that for XAD-4. The pore size distribution of Porapak Q has been reported to include pores of diameters from 30 to 400 Å, weighted more toward pores between 40 and 80 Å (Rixey, 1987). Amberlite XAD-4 should have a more uniform pore size distribution, centered around a pore size with a diameter of 100 Å (Albright, 1986). These figures could explain a factor of perhaps three difference in relative rates. Another possible rationalization for a lower effective diffusivity would be that Porapak Q has more blocked pores than XAD-4, and therefore has a higher tortuosity.

The sharpness of the leading edge of the experimental breakthrough data for acetic acid in Figure 4 could perhaps result from relatively faster diffusion within a fraction of the pores of Porapak Q characterized by a diameter similar to the pore diameter of XAD-4.

Acknowledgment

This research was supported by a grant from CPC International, Inc., and by the Assistant Secretary for Conservation and Renewable Energy, Office of Energy Systems Research, Energy Conversion and Utilization Technologies (ECUT) Division, U.S. Department of Energy, under Contract No. DE-AC03-76SF00098.

Notation

C = solute concentration
C_o = solute concentration in feed
d_p = particle diameter
D_f = diffusivity in fluid phase
D_L = effective axial diffusivity
D_p = effective diffusivity within particle
$F(t)$ = function, Eq. 3
I_o = modified Bessel function of zero order
k = lumped rate constant, s^{-1}
k_f = external mass-transfer coefficient at particle surface
K = partition coefficient or slope of equilibrium isotherm, m^3 interstitial fluid/m^3 adsorbent particles
N = number of transfer units, Eq. 6
Pe_b = bed Peclet number
Pe_p = particle Peclet number
R_p = particle radius
t = time since start of run
u = dummy variable, Eq. 3
v = interstitial fluid velocity
z = bed height
ϵ = porosity of bed

Literature Cited

Abe, I., K. Hayashi, and T. Hirashima, "Adsorption of Organic Compounds from Aqueous Solution onto Hydrophobic, High-Surface-Area Copolymer," *J. Colloid Interf. Sci.*, **94**, 577 (1983).

Albright, R. L., "Porous Polymers as an Anchor for Catalysis," *Reactive Polymers*, **4**, 155 (1986).

Glueckauf, E., and J. I. Coates, "Theory of Chromatography. IV: The Influence of Incomplete Equilibrium on the Front Boundary of Chromatograms and on the Effectiveness of Separation," *J. Chem. Soc.*, 1315 (1947).

Hasanain, M. A., and A. L. Hines, "Application of the Adsorption Potential Theory to Adsorption of Carboxylic Acids from Aqueous Solutions onto a Macroreticular Resin," *Ind. Eng. Chem. Process Des. Dev.*, **20**, 621 (1981).

Lapidus, L., and N. R. Amundson, "Mathematics of Adsorption in Beds. VI: The Effect of Longitudinal Diffusion in Ion Exchange and Chromatographic Columns," *J. Phys. Chem.*, **56**, 984 (1952).

Rixey, W. G., "Nonwet Adsorbents for the Selective Recovery of Polar Organic Solutes from Dilute Aqueous Solution," Ph.D. Diss. Dept. Chem. Eng., Univ. California, Berkeley (1987).

Rixey, W. G., and C. J. King, "Nonwetting Adsorbents for the Recovery of Solutes from Dilute Aqueous Solutions," *Fundamentals of Adsorption*, A. I. Liapis, ed., Engineering Foundation, New York, 503 (1987).

———, "Wetting and Adsorption Properties of Hydrophobic Macroreticular Polymeric Adsorbents," *J. Colloid Interf. Sci.*, in press (1988).

Ruthven, D. M., *Principles of Adsorption and Adsorption Processes*, Wiley, New York (1984).

Sherwood, T. K., R. L. Pigford, and C. R. Wilke, *Mass Transfer*, McGraw-Hill, New York (1975).

Manuscript received Mar. 2, 1988, and revision received Aug. 9, 1988.